An ab Initio Study of the Absorption Spectra of Indirubin, Isoindigo, and Related Derivatives

Eric A. Perpète,[†] Julien Preat, Jean-Marie André, and Denis Jacquemin*,[†]

Laboratoire de Chimie Théorique Appliquée, Facultés Universitaires Notre-Dame de la Paix, rue de Bruxelles, 61, B-5000 Namur, Belgium

Received: January 4, 2006; In Final Form: March 13, 2006

The UV/visible spectra of a series of indirubin, isoindigo, and other indigo/thioindigo related dyes have been evaluated in various solvent environments by using the time-dependent density functional theory in conjunction with the polarizable continuum model. Even for molecules of the same family, significant differences in the excitation processes have been noted. Two hybrid functionals have been selected: B3LYP and PBE0. For a set of the 50 selected molecular cases, both functionals provide accurate λ_{max}, with mean absolute deviations limited to 0.1 eV. Actually, isoindigo is the main challenging series, with systematically underestimated excitation energies, due to the different nature of the excitation process. In most cases, we found that PBE0 is more efficient in reproducing the experimental values than B3LYP for sulfur-containing dyes not featuring internal hydrogen bonds, the reverse assertion being also true. In addition, the spectra of a series of unknown dyes have been predicted.

I. Introduction

Known since antiquity, indigo (Figure 1) is still the most widely used blue-jeans dye with a world production approaching 15 000 tons/year. Since the seminal works of Bayer[1] and Heumann,[2,3] many artificial indigos have been synthesized though several derivatives of indigo are naturally occurring. Further chemical modifications lead to two major categories. On the one hand, one substitutes the phenyl rings with electroactive groups,[4−7] and on the other hand, one can intrinsically modify the nature of the indigo chromophore. A typical example is thioindigo (Figure 1), which was first reported by Friedländer at the beginning of the 20th century.[8,9] In this second category, one also finds mixed indigo−thioindigo compounds (**VI**), as well as molecules formed by bonding the two parts of indigo in several ways, for example, indirubin (**IV**) and isoindigo (**V**) (see Figure 2). Though indirubin was an important component of some antique dye,[10,11] most of these dyes have only been synthesized and identified about one century ago,[12−18] and some of its derivatives are still the subject of active research in the biochemical, phytochemical, or medical fields.[19−24] However, to our knowledge, no previous ab initio study of the excited-state spectra of these compounds has been performed.

This work aims at predicting and rationalizing the λ_{max} of indirubin, isoindigo, and other indigo derivatives (Figure 2) by gaining chemical insights explaining the spectral differences between various members of the indigo family. To reach this goal, we use time-dependent density functional theory (TD-DFT),[25] which is often found to be a robust and accurate method for describing low-lying excited states.[26−28] TD-DFT has been successfully used in a wide variety of (bio-) chemical and physical problems.[29−34] The typical errors on the excited-state energies reported by TD-DFT investigations strongly depend on the type of chromophoric unit, on the nature of the excitation studied (low-lying versus Rydberg, $n \rightarrow \pi^*$ versus $\pi \rightarrow \pi^*$, ...), and on the selected computational procedure (functional, basis set, solvent effects, statistical corrections, ...). Nevertheless, one can broadly state that hybrid functionals, which incorporate a fraction of exact exchange, are more successful than pure functionals. The amount of exact exchange included in the functional could vary, but it turns out that a percentage between 20% and 25% is often adequate for organic conjugated compounds. For instance, two of the most popular hybrids, B3LYP[35] and PBE0,[36] include one-fifth and one-fourth of Hartree−Fock exchange, respectively. Therefore, if one restricts itself to TD-DFT(hybrid) investigations of the few first $\pi \rightarrow \pi^*$ transitions in organic chromogens, one typically gets a mean absolute error (MAE) close to 0.2 eV with respect to experimental data. Indeed, (1) for the 22 substituted indigo compounds reported in ref 37, for which experimental values are given by the authors, one finds MAE = 0.23 eV; (2) for 100 sulfur-containing compounds, Fabian got a MAE of 0.24 eV with TD-B3LYP, i.e., significantly more accurate than with the ZINDO approach (0.40 eV);[38] (3) the same author obtained a MAE of 0.29 eV for a series of sulfur-free chromogens;[39] (4) for the first transitions in the 11 thiouracil compounds from ref 40, the MAE is 0.24 eV; (5) Jamorski and Casida found experimental versus theoretical absorption energy differences ranging between 0.10 and 0.30 eV for alkyl-amino-benzonitrile compounds.[41] However, studies explicitly accounting for bulk solvent effects and focusing on a given family of chromophores have achieved (much) better accuracy.[42,43] More specifically, for an extended set of substituted indigo compounds we obtained a MAE of 0.02 eV,[44] by using B3LYP;[35] whereas for 100 thioindigo derivatives, we found a MAE of 0.03 eV,[45,46] with the PBE0 functional.[36] Of course these remarkably small errors

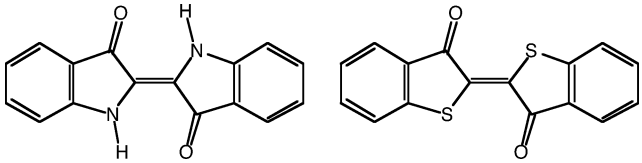

Figure 1. Sketch of indigo (left) and thioindigo (right).

* Author to whom correspondence should be addressed. E-mail: denis.jacquemin@fundp.ac.be. URL: http://perso.fundp.ac.be/~jacquemd.

[†] Research Associate of the Belgian National Fund for Scientific Research.

10.1021/jp060069e CCC: $33.50 © 2006 American Chemical Society
Published on Web 04/14/2006

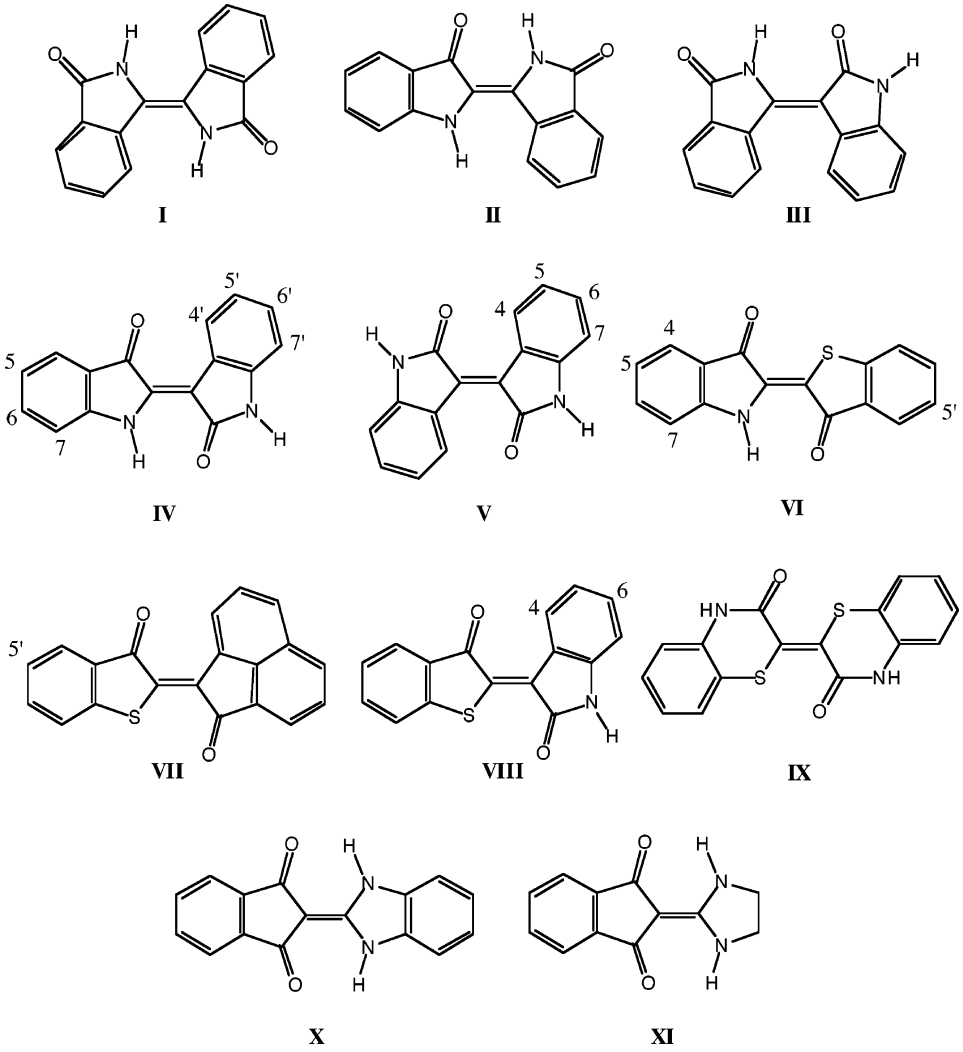

Figure 2. Sketch of the compounds studied in the first part of this work. **IV** is indirubin, **V** isoindigo, and **VII** vat scarlet G.

originate not only from the inclusion of solvent effects and the use of quite extended basis sets but also from an "optimal" choice of the functional, i.e., B3LYP (PBE0) would probably give larger a MAE for thioindigo (indigo). But three major questions remain: (1) What are the characteristics of the chromophore that should be taken into account for selecting a functional? (2) Which functional to choose? (3) For which case? Preliminary answers to these questions can be obtained by studying molecules derived from the indigo and thioindigo structures (see section III.A). Once a correct methodology is established, one can investigate the excitation processes related to the λ_{max} (see section III.B) but also predict the spectra of new structures (see section III.C). Therefore, in this contribution, we claim not only to accurately reproduce the λ_{max} of the investigated molecules and to unravel the excitation processes responsible for the color of the dyes sketched in Figure 2 but also to gain insights for the choice of the functional in TD-DFT, at least for indigo-derived dyes.

II. Computational Details

All calculations have been performed with the Gaussian03 suite of programs.[47] Except when noted, default thresholds and algorithms have been used. We have used a three-step methodology: (1) an optimization of the ground-state structure; (2) an analytic determination of the vibrational spectrum in order to check the absence of imaginary frequencies; (3) the evaluation of the electronic excited states. For all compounds in sections III.A and III.B, two separate calculations have been performed, one with the B3LYP hybrid functional,[35] and one with the parameter-free PBE0 functional.[36] During all calculations the SCF convergence criteria have been tightened to 10^{-10} au.

For each molecule, the ground-state structure has been determined using a TIGHT threshold, implying residual mean square (RMS) residual forces smaller than 1×10^{-5} au at the end of the minimization process. These optimizations have been performed with the 6-311G(d,p) basis set. This basis set has been found to yield valid geometries for both indigo[44] and thioindigo.[45]

The vibrational frequencies have been evaluated by the analytical determination of the Hessian matrix using the same level of theory with the same basis set as in the first step. Except when noted, no imaginary frequency has been detected in the theoretical vibrational spectra.

The visible absorption spectrum of each molecule and, more specifically, the wavelength of maximum absorption (λ_{max}) have been obtained by calculation of the ground/singlet-excited-state transition energy. These TD-DFT calculations have been performed with the 6-311+G(2d,p) basis set, which provides converged λ_{max} for dyes of the same chemical family;[44,45] i.e., further extension of the basis set is not expected to significantly affect the computed λ_{max} for this class of molecules. The excitations responsible for the color of indigo compounds

present a $\pi \rightarrow \pi^*$ character with a large oscillator force, and the reported λ_{max} always corresponds to the transition energy to the first dipole-allowed excited state with a significantly large transition probability.

At each stage, the bulk solvent effects are evaluated by means of the polarizable continuum model (IEF-PCM).[48] In PCM, one divides the model into a solute part, the dye, lying inside a cavity, surrounded by the solvent part, for example, benzene, cyclohexane, xylene,[49] chloroform, tetrachloroethane (TCE),[50] ethanol (EtOH), dimethyl sulfoxide (DMSO), or dimethylformamide (DMF),[51] represented as a structureless material, characterized by its macroscopic properties. PCM returns valid solvent effects when no specific interactions (such as hydrogen bonds) link the solute and the solvent molecules. Thanks to the latest algorithmic and methodological developments, the PCM approach can be applied for most properties (including excited states) at a reasonable computational cost compared to gas-phase calculations. In this paper we have selected the so-called nonequilibrium PCM solutions for the study of absorption processes.[30]

III. Results

A. Hybrid Functional Selection. The theoretical and experimental λ_{max} of the compounds sketched in Figure 2 are compared in Table 1. We note that significant discrepancies may appear between the values reported by different experimentalists, in which case we use an average value, except when noted. For instance, for indirubin in TCE, there is a 10 nm shift between Saddler's[52] and Clark's[53] λ_{max}. The 561 nm for **IV** in xylene[5] also seems doubtful in light of the more recent result in the very similar benzene (551 nm).[54] Furthermore, the 545 nm λ_{max} for **VIII** in xylene looks incorrect in light of the values found in benzene[54] (a 40 nm shift is nonrealistic). Therefore, the Formanek's values for **VIII** and its bromo derivative have not been used in the following, since we judged them (highly) questionable. This stresses that, on the one hand, available experimental data are not error-free and, on the other hand, comparisons with the spectra computed with TD-DFT have to be performed with care.

For the complete indirubin (**IV**) series, we obtain a mean signed error (MSE) on λ_{max} of −2 nm and −21 nm with B3LYP and PBE0, respectively, the theory (especially with PBE0) overestimating the excitation energy. The corresponding mean absolute errors are 8 nm (0.03 eV) and 21 nm (0.09 eV) for B3LYP and PBE0, respectively, clearly indicating that the former is highly competitive for indirubin, as it was for indigo. This is also confirmed by the largest discrepancies that amount to −20 nm and −38 nm, for B3LYP and PBE0, respectively. For both functionals, the extreme deviation corresponds to the 6,6′-Br-**IV**, for which the experiment is a bit outdated (1912). The largest experimental shifts (5-Br,7-Me- and 5,5′,7,7′-Br-**IV**) are also reasonably estimated by TD-DFT. To summarize, indirubin behaves like indigo, with tiny spectral shifts and a more accurate description by the B3LYP functional.

Contrary to the indirubin series, both B3LYP and PBE0 always overestimate the λ_{max} of isoindigos (**V** series) with respective MAE (or MSE) of +50 nm and +32 nm. The corresponding eV MAEs are quite large: 0.24 and 0.16 eV, respectively. Particularly, the 4-Me substitution leads to a hypsoshift of −30 nm in the experiment,[52] but to a mere +8/+9 nm bathoshift with TD-DFT. These larger errors could be related to significant modifications in the electronic density localization during the absorption (see next section).[55,56] Although the MAEs fall in the typical range of TD-DFT studies on organic molecules (see Introduction), the visible spectra of isoindigo dyes are poorly evaluated by TD-DFT compared to other indigo derivatives, especially when the B3LYP functional is selected. Consequently, for the **I**−**V** DMSO series from Wille and Lüttke,[57] TD-DFT predicts the following ordering for the λ_{max} (in nm):

I < **III** < **II** < **V** < **IV**

whereas the actual order is

I < **III** < **V** < **II** < **IV**

In addition, TD-DFT underestimates the isoindigo−indirubin shift by a factor close to 10/3, whereas for the other members of the series, these shifts are adequately reproduced by theory. For instance, going from **I** to **II** (**III**) gives an experimental shift of +103 nm (+44 nm) that is correctly returned by both B3LYP, +101 nm (+59 nm), and PBE0, +95 nm (+49 nm).

TABLE 1: Comparison between PCM-X/6-311+G(2d,p)// PCM-X/6-311G(d,p) and Experimental λ_{max} (nm) for the Compounds of Figure 2

substituent	solvent	X = B3LYP	X = PBE0	expt	ref
I	DMSO	405	395	413	57
II	DMSO	506	490	516	57
III	DMSO	464	444	455	57
IV	xylene	546	528	561	5
	TCE	551	532	550/540	52/53
	DMSO	556	536	551	57
	benzene	546	528	551	54
	DMF	555	536	546	63
5-Br,7-Me-**IV**	xylene	569	551	582	5
5,5′,7,7′-Br-**IV**	xylene	574	554	579	5
4′-Me-**IV**	TCE	550	530	552	52
4′-CF3-**IV**	TCE	551	532	548	52
5′-Me-**IV**	TCE	560	539	552	52
6-Br-**IV**	TCE	548	528	558	53
6,6′-Br-**IV**	xylene	547	529	567	64
	TCE	549	532	552	53
6′-Me-**IV**	TCE	557	539	550	52
6′-Cl-**IV**	TCE	554	536	568	52
6′-Br-**IV**	TCE	555	537	538	53
7′-Me-**IV**	TCE	554	534	555	52
V	TCE	533	515	485	52
	DMSO	537	519	491	57
	benzene	525	507	478	54
4-Me-**V**	TCE	542	523	455	52
6-Me-**V**	TCE	533	516	495	52
6-Cl-**V**	TCE	535	517	485	52
6-OMe-**V**	TCE	532	515	505	52
7-F-**V**	TCE	534	515	485	52
7-Me-**V**	TCE	539	520	480	52
VI	$CHCl_3$	576	558	579	12
	xylene	574	556	575	5
	benzene	574	556	574	54
5-Br-**VI**	xylene	589	570	583	5
	benzene	589	570	584	54
5,5′-Br-**VI**	xylene	597	578	589	5
	benzene	597	578	590	54
5,7-Br-**VI**	xylene	594	575	584	5
5,5′,7-Br-**VI**	xylene	603	584	590	5
4,5,7-Br-**VI**	xylene	595	576	586	5
VII	xylene	534	515	517	5
	cyclohexane	532	513	508	54
	benzene	534	515	514/512	65/54
	EtOH	536	516	510	66
5′-Br-**VII**	xylene	549	529	521	5
	cyclohexane	547	528	517	54
	benzene	549	529	517	54
VIII	xylene	536	517	545	5
	benzene	536	517	505	54
4,6-Br-**VIII**	xylene	540	522	544	5
IX	DMSO	463	447	450	67
X	methanol	335	325	355	68
XI	methanol	294	285	318	68

TABLE 2: Mean Absolute Error (MAE) (nm and eV) for Different Sets of Compounds Extracted from Table 1[a]

	nm		eV	
	B3LYP	PBE0	B3LYP	PBE0
total	19 (12)	19 (16)	0.09 (0.06)	0.10 (0.08)
internal H-bonds	9 (9)	19 (19)	0.03 (0.03)	0.09 (0.09)
no internal H-bonds	36 (23)	19 (8)	0.17 (0.11)	0.10 (0.04)
sulfur containing	15 (15)	10 (10)	0.06 (0.06)	0.04 (0.04)
no sulfur	21 (10)	25 (22)	0.11 (0.06)	0.13 (0.12)

[a] The values in parentheses correspond to the results obtained when isoindigos are discarded from the statistical analysis.

For the half-indigo−half-thioindigo series, **VI**, we obtained MSEs of 5 nm and −13 nm and MAEs of 6 nm (0.02 eV) and 13 nm (0.05 eV), with B3LYP and PBE0, respectively. Often, the experimental values are bracketed by the results of the two hybrids, and the spectral shifts are nicely reproduced. Although PBE0 still gives extremely good results, B3LYP is more accurate for these half-and-half structures. On the contrary, for **IX**, which also contains NH groups and sulfur atoms, PBE0 is on the spot.

To obtain a more general picture, we report in Table 2 the MAEs obtained for the complete set of molecules included in Table 1. Overall the total MAEs are completely comparable for the two functionals and are limited to 0.1 eV, although several isoindigo compounds are present in the set. By removing the **V** series from the statistics, one gets MAEs of 0.06 and 0.08 eV for B3LYP and PBE0, respectively. If one considers only molecules with internal hydrogen bonds (**II**, **III**, **IV**, **VI**, **X**, and **XI**), the MAE of PBE0 is unchanged but B3LYP performs significantly better (0.03 eV). The drawback is that B3LYP is a bit less efficient for H-bond-free structures (0.17 eV). For sulfur-containing molecules, the MAEs are smaller (in part due to the removal of isoindigo from the statistics), especially for PBE0 (0.04 eV). These results are completely consistent, on the one hand, with the fact that B3LYP is favored for indigo,[44] and PBE0 for thioindigo,[45,46] and, on the other hand, with our 2004 study of 9,10-anthraquinones.[58] Indeed, in that work, we found that PBE0 was generally more efficient, except for anthraquinones with amino derivatives in 1, 4, 5, and/or 8 positions (i.e., in positions where hydrogen bonds can be formed between the side N−H groups and the central carbonyl moieties). For these latter anthraquinones, B3LYP gave more accurate values.

B. Analysis of Spectral Differences. Indirubins (**IV**) always show a symmetry close to the C_s point group, except for 4′-Me and 4′-CF_3, which significantly deviate from planarity due to huge steric effects. In these two latter dyes, the bridge dihedral angles lie between 15° and 20° (B3LYP and PBE0 dihedral angles are similar), but the fused rings on either sides of the molecules remain mainly planar. A test calculation with the bulky 4′-tBu reveals both a slightly increased central dihedral angle and a less planar conjugated ring. For **IV**, the excitation responsible for the color typically corresponds to the HOMO → LUMO transition, as in most indigos. The shapes of these frontier orbitals were obtained with the B3LYP functional and are depicted in Figure 3. They are typical of $\pi \rightarrow \pi^*$ transitions with densities going from the central double bond to the side single bonds. Compared to indigo,[44] the HOMO presents a significant electron density in one of the phenyl rings, whereas the LUMO is still centered on the five-membered rings. Experimental studies have demonstrated that, for indirubins, the substitution of the outer phenyl rings often leads to negligible spectral shifts.[52] This effect, well reproduced by TD-DFT, can be related to the relatively minor role played by the six-membered rings in the frontier orbitals.

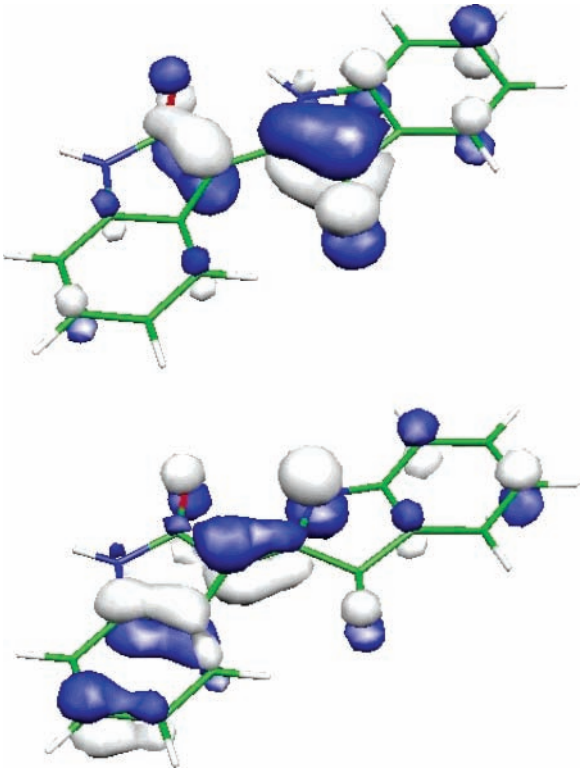

Figure 3. HOMO (bottom) and LUMO (top) of **IV** obtained with PCM(DMSO)-B3LYP/6-311+G(2d,p).

Isoindigo (**V**) is a nonplanar molecule belonging to the C_2 point group. The inter-ring dihedral angle is close to 15° and is mostly unchanged by the substitution, except for 4-Me, which gives a stronger steric hindrance, and increases the twist to about 23°. For **V** in benzene, imposing the planarity would lead to an increase of the total energy by 0.4−0.5 kcal/mol and a bathoshift estimated to +8 nm with PBE0, indicating that the nonplanarity has only a small intrinsic impact on the first excited state energy. For all these compounds, the λ_{max} also corresponds to the HOMO to LUMO transition though a small HOMO-2 → LUMO contribution shows up. These molecular orbitals are depicted in Figure 4. While the LUMO is similar to that of indigo,[44] the HOMO and HOMO−2 are much more delocalized with major contributions on the outer phenyl rings. Therefore, the actual chromophoric unit is no more centered on the five-membered rings as it was in the case for (thio)indigo,[44,46,59−61] and the actual excitation shows a charge-transfer character (from the phenyl rings to the central moiety). This explains the stronger benzene−DMSO solvatochromic effect in **V** than in **IV** and can also be related to the important TD-DFT errors found for isoindigo. Indeed, large theory/experiment discrepancies are often reported when significant changes in the electronic density localization appear during the absorption:[55,56] for this type of excitation, it is known that (TD-)DFT tends to undershoot the transition energies.[38,62]

For the remaining components of the Wille and Lüttke series,[57] i.e., **I**, **II** and **III**, we have found nonplanar structures belonging to the C_2, C_1, and C_1 point groups, respectively. For **I**, the central N−C−C−N dihedral angle is close to 170° with a gain of stability of 0.6 kcal/mol (and a +6 nm λ_{max} displacement) compared to the planar structure. For **II**, the structure is almost perfectly planar, except for the hydrogen bound to the "bottom" nitrogen (see Figure 2), which goes out of the plane to prevent repulsive interactions with the right-

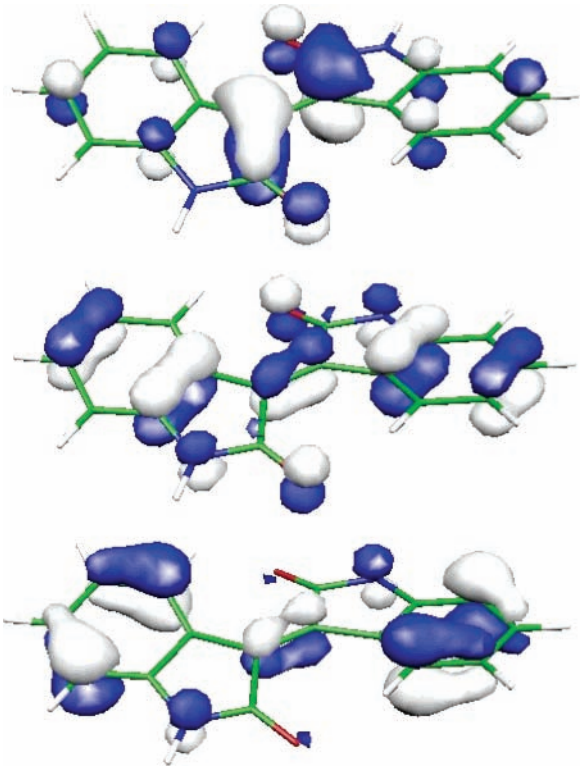

Figure 4. HOMO−2 (bottom), HOMO (center), and LUMO (top) of **V**. These pictures have been obtained with PCM(DMSO)-PBE0/6-311+G(2d,p).

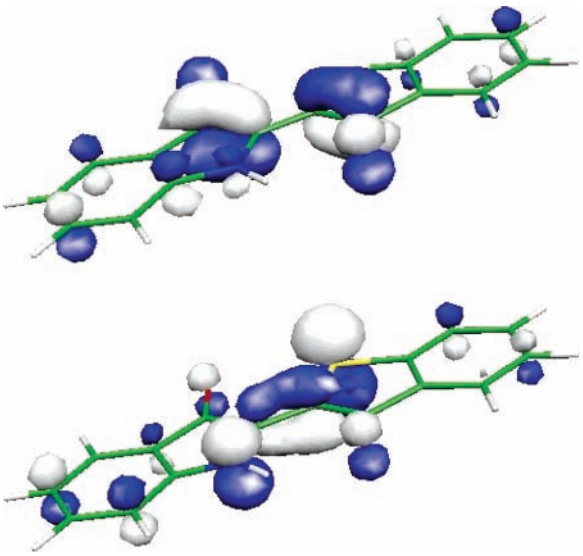

Figure 5. HOMO (bottom) and LUMO (top) of **VI** obtained with PCM($CHCl_3$)-B3LYP/6-311+G(2d,p).

hand-side phenyl ring. Forcing a C_s ground state leads to an increase of total energy by 0.4 kcal/mol and a +16 nm bathoshift. For **II**, the most stable structure is drawn in Figure 2, with the two benzene rings on the same side of the dye in order to allow a stabilizing hydrogen bond between the carbonyl and the amine groups. These latter groups are coplanar although the aromatic rings are distorted in the same fashion as in helicenes. The gain in energy compared to the structure drawn in ref 57 (without H-bond but with non-interacting phenyl rings) is significant (1.1 kcal/mol), although the impact on the UV/vis spectrum is limited.

The molecules with one indigo half and one thioindigo half (**VI**) present only one hydrogen bond, but this bond is strong

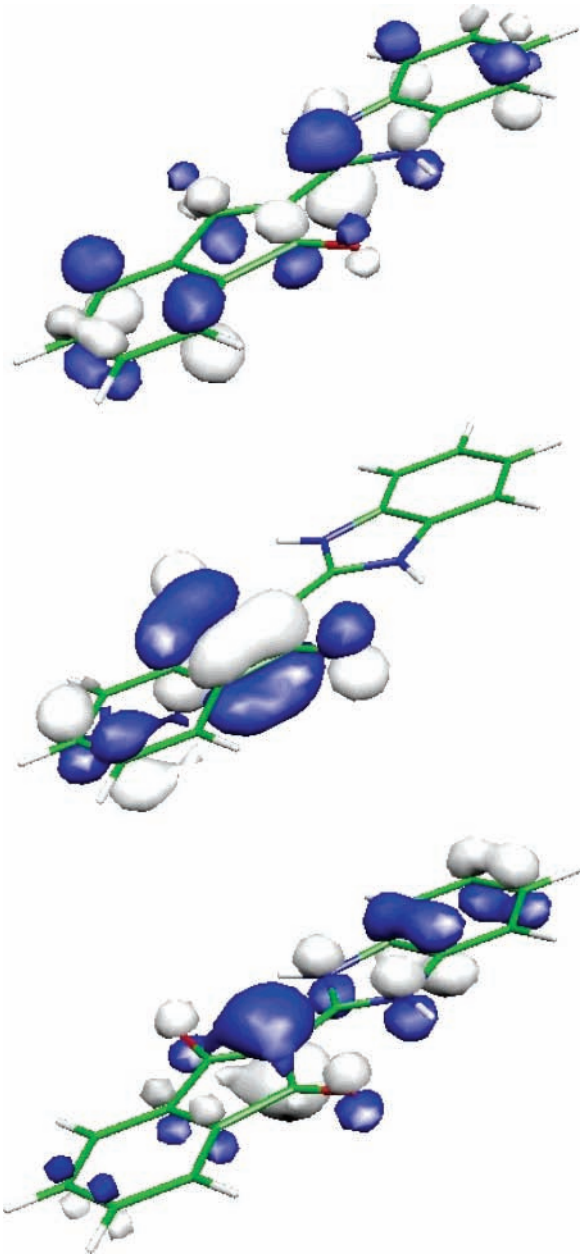

Figure 6. HOMO (bottom), LUMO (center), and LUMO+1 (top) of **X** obtained with PCM(MeOH)-B3LYP/6-311+G(2d,p).

enough to prevent the trans−cis isomerization occurring in thioindigo.[54] They have been found planar, as their parent dyes. The two frontier orbitals that play a role in the color of derivatives are depicted in Figure 5 and are completely equivalent to their indigo and thioindigo counterparts,[44,46] i.e., they are well localized, which is the "best" case for TD-DFT. This explains the quality of the results obtained in section III.A.

X looks similar to indigo (same stoichiometry, number of π electrons, number of hydrogen bonds, and so on) but presents a vertical excitation energy that is almost twice as large. At first sight, it could be understood by the change in symmetry, which makes the HOMO → LUMO transition forbidden, and would explain this tremendous enhancement. Indeed, the 335 nm (B3LYP) peak corresponds to a HOMO → LUMO+1 excitation. Nevertheless the HOMO → LUMO transition takes place at 416 nm (B3LYP), still far from the indigo value (around 600 nm in polar solvents). All these frontier orbitals are shown in Figure 6. The HOMO is not centered on the bridge double bond as in indigo[44] and, furthermore, presents a large contribu-

TABLE 3: Prediction of the λ_{max} (nm) for the Compounds of Figure 7

compound	solvent	functional	λ_{max}
XII	DMSO	PBE0	402
XIII	DMSO	PBE0	405
XIV	DMSO	B3LYP	491
XV	DMSO	PBE0	483
XVI	xylene	PBE0	527
XVII	MeOH	B3LYP	354
XVIII	MeOH	PBE0	372
XIX	MeOH	B3LYP	309
XX	MeOH	PBE0	330

tion on one of the phenyl rings. On the contrary, the LUMOs of indigo and **X** are similar but for their symmetry, while the LUMO+1 is delocalized over the whole structure and presents numerous nodes.

C. New Structures. In Table 3, we have predicted the spectra of the unknown species represented in Figure 7. The functionals used during these calculations have been determined following the conclusions of section III.A, i.e., B3LYP has been selected for compounds presenting an amine−carbonyl hydrogen bond, whereas PBE0 has been chosen in the other cases. Note that none of the dyes of Figure 7 are sulfur-free as these structures were found to be the most problematic for our approach. Therefore, we believe that the values reported in Table 3 can be trusted both qualitatively and (almost) quantitatively.

For **XII** and **XIII**, the distortion of the bridge dihedral angle is completely similar to that of **I**, and we predict a small bathoshift (+10 nm) when replacing both amine groups by sulfur atoms, as expected for H-bond-free molecules. Contrary to **II**, **XIV** and **XV** have a planar C_s ground state. We predict a small hypsoshift when adding sulfur atoms in **II**, stressing the importance of H-bonds in that structure.

In the series **X** → **XVII** → **XVIII** (and **XI** → **XIX** → **XX**), one notes a systematic bathoshift (∼+20 nm at each step), which is exactly the opposite behavior noted (experimentally and theoretically) for the indigo → **VI** → thioindigo series. This clearly originates in the different excitation processes in indigo and in **X** (see section III.B). In addition, it shows that the impact of the hydrogen bonds on the UV/vis spectra is much weaker in **X** than in indigo, as removing such interactions by adding a softer sulfur atom systematically leads to a bathoshift in the former (hypsoshift in the latter).

IV. Conclusion and Outlook

Using a PCM-TD-DFT/6-311+G(2d,p)//PCM-DFT/6-311G-(d,p) approach combined with two hybrid functionals, we have computed the first $\pi \rightarrow \pi^*$ excitation energies of a series of indigos. The problematic case of isoindigo left aside, this approach is very successful in quantitatively reproducing the λ_{max} of absorption of these dyes, as well as the evolution of the spectra induced by chemical substitutions on the rings or changes of the chromophoric moiety. Indeed, without isoindigo, the MAEs are 0.06 and 0.08 eV for B3LYP and PBE0, respectively, significantly smaller than the typical 0.20 eV TD-DFT error reported for the first dipole-allowed transitions of organic dyes. Furthermore, the present investigation suggests that B3LYP (PBE0) can be favored for compounds characterized by at least one (no) strong internal hydrogen bond with the carbonyl groups. Such a hint is also supported by the results from our previous investigation on anthraquinones. In addition, it appears that sulfur-containing indigos are better described with PBE0. The difficulty to accurately reproduce the spectra of isoindigo with TD-DFT could be explained by the excitation process which significantly differs from the other members of the series. This work demonstrates that qualitative descriptions of the excitation processes, which help in rationalizing spectral differences between similar dyes, can often be combined with nearly-quantitative procedures, allowing an efficient color-chemistry design.

We are currently investigating the transferable character of these conclusions to dyes not belonging to the indigo or anthraquinone families.

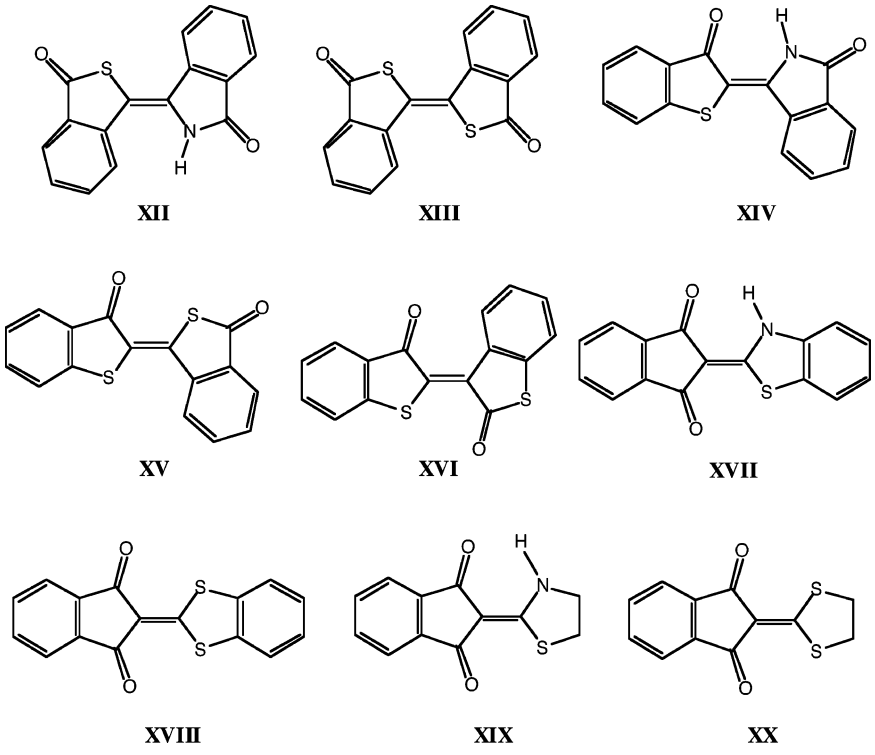

Figure 7. Sketch of the compounds used in Table 3.

Acknowledgment. D.J. and E.A.P. thank the Belgian National Fund for Scientific Research for their research associate positions. J.P. acknowledges the FRIA (Belgian "Fonds pour la formation la Recherche dans l'Industrie et dans l'Agriculture") for his Ph.D. grant. Most calculations have been performed on the Interuniversity Scientific Computing Facility (ISCF), installed at the Facultés Universitaires Notre-Dame de la Paix (Namur, Belgium), for which the authors gratefully acknowledge the financial support of the FNRS-FRFC and the "Loterie Nationale" for the convention number 2.4578.02 and of the FUNDP.

References and Notes

(1) Baeyer, A.; Drewson, V. *Ber. Dtsch. Chem. Ges.* **1882**, *15*, 2856−2864.
(2) Heumann, K. *Chem. Ber.* **1890**, *23*, 3043−3045.
(3) Heumann, K. *Chem. Ber.* **1890**, *23*, 3431−3435.
(4) Friedländer, P.; Bruckner, S.; Deutsch, G. *Justus Liebigs Ann. Chem.* **1912**, *388*, 23−49.
(5) Formanek, J. *Angew. Chem.* **1928**, *41*, 1133−1141.
(6) Gindraux, L. *Helv. Chim. Acta* **1929**, *12*, 921−934.
(7) Saddler, P. W. *J. Org. Chem.* **1956**, *21*, 316−318.
(8) Friedländer, P. *Ber. Dtsch. Chem. Ges.* **1906**, *39*, 1060−1069.
(9) Friedländer, P. *Justus Liebigs Ann. Chem.* **1907**, *351*, 390−420.
(10) Clark, R. J. H.; Cooksey, C. J. *New J. Chem.* **1999**, *1999*, 323−328.
(11) Cooksey, C. J. *Molecules* **2001**, *6*, 736−769.
(12) Friedländer, P. *Ber. Dtsch. Chem. Ges.* **1908**, *41*, 772−777.
(13) Wahl, A.; Bagard, P. *Bull. Soc. Chim. Fr.* **1910**, *5*, 1043−1045.
(14) Wahl, A.; Bagard, P. *Bull. Soc. Chim. Fr.* **1911**, *7*, 1090−1101.
(15) Wahl, A.; Bagard, P. *Bull. Soc. Chim. Fr.* **1914**, *15*, 329−336.
(16) Wahl, A.; Bagard, P. *Bull. Soc. Chim. Fr.* **1914**, *15*, 336−342.
(17) Friedländer, P. *Ber. Dtsch. Chem. Ges.* **1922**, *55*, 1591−1596.
(18) Friedländer, P.; Sander, L. *Ber. Dtsch. Chem. Ges.* **1924**, *57*, 649−652.
(19) Maugard, T.; E., E.; Choisy, P.; Legoy, M. D. *Phytochemistry* **2001**, *58*, 897−904.
(20) Nam, S.; Buettner, R.; Turkson, J.; Kim, D.; Cheng, J. Q.; Muehlbeyer, S.; Hippe, F.; Vatter, S.; Merz, K. H.; Eisenbrand, G.; Jove, R. *Proc. Natl. Acad. Sci. U.S.A.* **2005**, *102*, 5998−6003.
(21) Bradbury, J. *Drug Discovery Today* **2005**, *10*, 1131−1132.
(22) Celik, A.; Speight, R. E.; Turner, N. J. *Chem. Commun.* **2005**, 3652−3654.
(23) Suzuki, K.; Adachi, R.; Hirayama, A. S.; Watanabe, H.; Otani, S.; Watanabe, Y.; Kasahara, T. *Br. J. Haematol.* **2005**, *130*, 681−690.
(24) Ye, B. X.; Yuan, L. J.; Chen, C.; Tao, J. C. *Electroanalysis* **2005**, *17*, 1523−1528.
(25) Runge, E.; Gross, E. K. U. *Phys. Rev. Lett.* **1984**, *52*, 997−1000.
(26) Casida, M. E. Accurate Description of Low-Lying Molecular States and Potential Energy Surfaces. In *Low-Lying Potential Energy Surfaces*; Hoffmann, M. R., Dyall, K. G., Eds.; ACS Symposium Series 828; American Chemical Society: Washington, DC, 2002.
(27) Onida, G.; Reining, L.; Rubio, A. *Rev. Mod. Phys.* **2002**, *74*, 601−659.
(28) Maitra, N. T.; Wasserman, A.; Burke, K. In *Electron Correlations and Materials Properties 2*; Gonis, A., Kioussis, N., Ciftan, M., Eds.; Kluwer: Dordrecht, 2003.
(29) Adamo, C.; Barone, V. *Chem. Phys. Lett.* **2000**, *330*, 152−160.
(30) Cossi, M.; Barone, V. *J. Chem. Phys.* **2001**, *115*, 4708−4717.
(31) Baerends, E. J.; Ricciardi, G.; Rosa, A.; van Gisbergen, S. J. A. *Coordin. Chem. Rev.* **2002**, *230*, 5−27.
(32) Jamorski-Jödicke, C.; Lüthi, H. P. *J. Am. Chem. Soc.* **2002**, *125*, 252−264.
(33) Zalis, S.; Ben Amor, N.; Daniel, C. *Inorg. Chem.* **2004**, *43*, 7978−7985.
(34) Improta, R.; Barone, V. *J. Am. Chem. Soc.* **2004**, *126*, 14320−14321.
(35) Becke, A. D. *J. Chem. Phys.* **1993**, *98*, 5648−5652.
(36) Adamo, C.; Barone, V. *J. Chem. Phys.* **1999**, *110*, 6158−6170.
(37) Xue, Y. S.; Gong, X. D.; Xiao, H. M.; He, T. *Acta Sin. Chim.* **2004**, *62*, 963−968.
(38) Fabian, J. *Theor. Chem. Acc.* **2001**, *106*, 199−217.
(39) Fabian, J.; Diaz, L. A.; Seifert, G.; Niehaus, T. *J. Mol. Struct. (THEOCHEM)* **2002**, *594*, 41−53.
(40) Shukla, M. K.; Leszczynski, J. *J. Phys. Chem. A* **2004**, *108*, 10367−10375.
(41) Jamorski-Jödicke, C.; Casida, M. E. *J. Phys. Chem. B* **2004**, *108*, 7132−7141.
(42) Hommen de Mello, P.; Mennucci, B.; Tomasi, J.; da Silva, A. B. F. *Theor. Chem. Acc.* **2005**, *113*, 274−280.
(43) Jacquemin, D.; Preat, J.; Perpète, E. A. *Chem. Phys. Lett.* **2005**, *410*, 254−259.
(44) Jacquemin, D.; Preat, J.; Wathelet, V.; Perpète, E. A. *J. Chem. Phys.* **2006**, *124*, 074104.
(45) Jacquemin, D.; Preat, J.; Wathelet, V.; Perpète, E. A. *J. Mol. Struct. (THEOCHEM)* **2005**, *731*, 67−72.
(46) Jacquemin, D.; Preat, J.; Wathelet, V.; Fontaine, M.; Perpète, E. A. *J. Am. Chem. Soc.* **2006**, *128*, 2072−2083.
(47) Frisch, M. J.; et al. *Gaussian 03*, revision B.04; Gaussian, Inc.: Wallingford, CT, 2004.
(48) Tomasi, J.; Mennucci, B.; Cammi, R. *Chem. Rev.* **2005**, *105*, 2999−3094.
(49) Xylene, as toluene except for EPS=2.27, RSOLV=3.01, VMOL=123.7, which have been set following available physicochemical data. Note that in the oldest experiments, the relative positions of the methyl groups (i.e., ortho, meta, or para) are not given. The above parameters correspond to *p*-xylene, which is used in the most recent experiments.
(50) 1,1′,2,2′-Tetrachloroethane, as 1,2-dichloroethane except for EPS=8.20, RSOLV=2.90, VMOL=105.2, which have been set following available physicochemical data.
(51) Dimethylformamide, as DMSO except for EPS=36.70, RSOLV=2.44, VMOL=69.6, which have been set following available physicochemical data.
(52) Saddler, P. W. *Spectrochim. Acta* **1960**, *16*, 1094−1099.
(53) Clark, R. J. H.; Cooksey, C. J. *J. Soc. Dyers Colour.* **1997**, *113*, 316−321.
(54) Haucke, G.; Paetzold, R. *Nova Acta Leopoldina Suppl.* **1978**, *11*, 1−123.
(55) Tozer, D. J. *J. Chem. Phys.* **2003**, *119*, 12697−12699.
(56) Dreuw, A.; Head-Gordon, M. *J. Am. Chem. Soc.* **2004**, *126*, 4007−4016.
(57) Wille, E.; Lüttke, W. *Chem. Ber.* **1973**, *106*, 3240−3257.
(58) Jacquemin, D.; Preat, J.; Charlot, M.; Wathelet, V.; André, J. M.; Perpète, E. A. *J. Chem. Phys.* **2004**, *121*, 1736−1743.
(59) Klessinger, M.; Lüttke, W. *Tetrahedron* **1963**, *19* (Suppl. 2), 315−335.
(60) Lüttke, W.; Klessinger, M. *Chem. Ber.* **1964**, *97*, 2342−2357.
(61) Klessinger, M.; Lüttke, W. *Chem. Ber.* **1966**, *99*, 2136−2145.
(62) Guillaumont, D.; Nakamura, S. *Dyes Pigm.* **2000**, *46*, 85−92.
(63) Seixas de Melo, J.; Moura, A.; Melo, M. J. *J. Phys. Chem. A* **2004**, *108*, 6975−6981.
(64) Ettinger, L.; Friedländer, P. A. *Ber. Dtsch. Chem. Ges.* **1912**, *45*, 2074−2080.
(65) Rogers, D. A.; Margerum, J. D.; Wyman, G. M. *J. Am. Chem. Soc.* **1957**, *79*, 2464−2468.
(66) Egerston, G. S.; Galil, F. *J. Soc. Dyers Colour.* **1962**, *78*, 167−176.
(67) Kaul, B. L. *Helv. Chim. Acta* **1974**, *57*, 2664−2678.
(68) Junek, H.; Fischer-Colbrie, H.; Sterk, H. *Chem. Ber.* **1977**, *110*, 2276−2285.